



# Three-dimensional electrode microbial fuel cell for hydrogen peroxide synthesis coupled to wastewater treatment



Jia-yi Chen, Nan Li\*, Lin Zhao<sup>1</sup>

Department of Environmental Science and Engineering, Tianjin University, Tianjin, China

## HIGHLIGHTS

- A three-dimensional electrode microbial fuel cell for H<sub>2</sub>O<sub>2</sub> synthesis is proposed.
- Graphite particle electrodes show the best performance on catalyzing H<sub>2</sub>O<sub>2</sub> synthesis.
- Micropores in granules provide additional ORR sites leading to a high power output.
- A relative high current has a positive impact on H<sub>2</sub>O<sub>2</sub> synthesis and COD removal.
- MFC with particle electrodes has superior ability of H<sub>2</sub>O<sub>2</sub> synthesis and COD removal.

## ARTICLE INFO

### Article history:

Received 14 November 2013

Received in revised form

11 December 2013

Accepted 30 December 2013

Available online 8 January 2014

### Keywords:

Hydrogen peroxide

Three-dimensional electrode

Microbial fuel cell

COD removal

## ABSTRACT

A three-dimensional electrode bioelectrochemical system for the cathodic production of hydrogen peroxide and the simultaneous treatment of wastewater is investigated. Three types of three-dimensional electrodes – activated carbon particle electrodes (ACPE), carbon black particle electrodes (CBPE) and graphite particle electrodes (GPE) – are made of activated carbon (AC), carbon black (CB) and graphite powders respectively with polytetrafluoroethene (PTFE) as the binder. The MFC using the GPE is shown to perform best for catalyzing H<sub>2</sub>O<sub>2</sub> production, while the MFCs equipped with the CBPE and the ACPE achieve a 17–18% higher power output but a 2.5–4.4% lower H<sub>2</sub>O<sub>2</sub> yield, due to the further cathodic reduction of H<sub>2</sub>O<sub>2</sub>. Furthermore, a relatively high current in the system is demonstrated to have a positive impact on both cathodic H<sub>2</sub>O<sub>2</sub> generation and anodic organic degradation for each MFC. At an external resistance of 20 Ω, the MFC using the GPE achieves the H<sub>2</sub>O<sub>2</sub> generation of 196.50 mg L<sup>-1</sup> and 84% COD removal in 24 h, with Coulombic efficiency, Faradic efficiency and COD conversion efficiency of 29%, 70%, and 20%, respectively. This study shows that MFC with carbon three-dimensional electrode is a cost-effective energy-saving bioelectrochemical system for the simultaneous production of hydrogen peroxide and removal of COD.

© 2014 Elsevier B.V. All rights reserved.

## 1. Introduction

Microbial fuel cells (MFCs) are a newly developed technology coupling electricity production with wastewater treatment [1,2]. Wastewater is used as a renewable resource to feed electrochemically active bacteria and generate electrons via the anode. These electrons are then transferred in the form of a current through an external circuit to the cathode and consumed by electron acceptors. Oxygen is a proven suitable and sustainable electron acceptor with a high oxidation potential and no production of secondary pollution

[3]. In the cathode chamber, oxygen reduction reaction (ORR) proceeds in four-electron or two-electron pathways on the cathode surface. When oxygen reduction by the four-electron reaction results in water production, the MFC typically generates a high current as well as a high power output. Alternatively, the oxygen can be reduced through a two-electron reaction, resulting in the formation of hydrogen peroxide (H<sub>2</sub>O<sub>2</sub>) [4]. Although the two-electron pathway is less efficient in the terms of power production, it provides a new method for synthesizing H<sub>2</sub>O<sub>2</sub> from wastewater [5].

Hydrogen peroxide is a strong chemical oxidant with many industrial wide-ranging uses, such as the bleaching of fiber in the textile industry, pulp bleaching and the deinking of paper products, and chemical synthesis [6]. In particular, H<sub>2</sub>O<sub>2</sub> is used in wastewater treatment for deodorizing, disinfecting and decolorizing wastewater [7]. Currently, the main method of H<sub>2</sub>O<sub>2</sub> production is

\* Corresponding author. Tel./fax: +86 22 27891291.

E-mail addresses: [nli@tju.edu.cn](mailto:nli@tju.edu.cn) (N. Li), [zhaolin@tju.edu.cn](mailto:zhaolin@tju.edu.cn) (L. Zhao).

<sup>1</sup> Tel./fax: +86 22 27890257.

the anthraquinone oxidation process, which has the disadvantages of potential toxicity and high operational costs [8,9]. In addition, cathodic  $\text{H}_2\text{O}_2$  can be electrochemically generated by oxygen reduction reaction using inexpensive carbon cathode materials (e.g., graphite, activated carbon, and carbon nanotubes) in chemical fuel cells [10,11] and electrochemical cells [12,13]. Several reports [14–17] have shown that it is possible to synthesize  $\text{H}_2\text{O}_2$  successfully in a MFC system without external power inputs, overcoming the high energy consumption problem of the electrochemical approach [12]. However, compared to electrochemical approaches, the synthesis process of MFCs has not performed as well as expected, with lower yields of  $\text{H}_2\text{O}_2$ . Fu et al. [14] produced  $\text{H}_2\text{O}_2$  in a MFC with a concentration of around  $80 \text{ mg L}^{-1}$  at rate of  $6.57 \text{ mg L}^{-1} \text{ h}^{-1}$ . Feng et al. [15] were the first to utilize a MFC generating Fenton's reagent at the cathode at a rate of about  $0.1 \text{ mg L}^{-1} \text{ h}^{-1}$ . Zhuang et al. [16] also investigated the MFC-Fenton system for *in situ* generation of  $\text{H}_2\text{O}_2$  at the cathode but only at a rate of  $0.014 \text{ mg L}^{-1} \text{ h}^{-1}$ .

It has been widely recognized that an increase in the electrode surface is important in the mass production of hydrogen peroxide. In this respect, a three-dimensional electrode is more attractive than a two-dimensional one because of its extensive interfacial electrode surface and high mass transfer [18]. In the three-dimensional electrode system, many small regular or random particles are stacked in the electric field forming charged micro-electrodes, called particle electrodes [19]. In addition, particle electrode materials are generally continuous in their porosities, large in specific surface area and high in electrical conductivity, contributing to an increased mass transfer coefficient [20] as well as enhanced energy production [21]. The literature indicates that the utilization of three-dimensional electrodes could lead to better performance in wastewater treatment [17,22,23]. As an environmental-friendly system, MFCs with three-dimensional electrodes could therefore be a novel, cost-effective, energy-saving technology for  $\text{H}_2\text{O}_2$  synthesis with simultaneous wastewater treatment.

In this study, MFCs equipped with three-dimensional cathodes were utilized to produce  $\text{H}_2\text{O}_2$  with simultaneous anodic organic degradation. Particle electrodes were developed using by various inexpensive carbon materials and the efficiency of these particle electrodes was studied. The operating parameters for the cathodic production of  $\text{H}_2\text{O}_2$  and anodic removal of COD in MFCs with three-dimensional cathodes were also investigated.

## 2. Experimental

### 2.1. Carbon particle electrodes fabrication

The particle electrodes were prepared according to the following procedures. Three carbon powders—activated carbon (designated AC,  $60 \mu\text{m}$ , Kewei Co. Ltd., Tianjin, China), carbon black (designated CB,  $30 \text{ nm}$ , Vulcan XC-72R, Cabot Corporation, USA), and graphite ( $30 \mu\text{m}$ , CAS#7782-42-5, Sinopharm Chemical Reagent Co. Ltd., Shanghai, China) — were pretreated by ultrasonic cleaning in deionized water for 30 min at  $30^\circ\text{C}$ . After drying, each sample of pretreated carbon powder was dispersed into an appropriate amount of ethanol in a beaker and stirred for 60 min at  $70^\circ\text{C}$ . Then  $75 \mu\text{L}$  of PTFE suspension ( $60 \text{ wt}\%$ , Hesen, Shanghai, China) per gram of carbon powder were dripped into the mixture slowly in a  $70^\circ\text{C}$  bath, and the carbon and PTFE particles were distributed by stirring, in order to form extensive networks of gas channels, until the blend became a dough-like paste [24]. The paste was rolled using extrusion-spheronization technology to produce carbon-PTFE granules for use as particle electrodes (sampled as ACPE, CBPE, and GPE in turn) with a diameter of 2–3 mm.

### 2.2. Material characterization of carbon particle electrodes

Images of the surface morphology of the carbon powders and the corresponding carbon-PTFE granules were taken with a scanning electron microscope (SEM, Nanosem 430, USA). A nitrogen adsorption/desorption (BET) analysis was performed at  $77 \text{ K}$ , using Autosorb-1 (Quantachrome, USA), to identify the specific surface areas of the carbon-PTFE granules. Porous properties and the pore size distribution of the samples were analyzed using the BJH model.

### 2.3. MFC configuration and operation

The experiments were performed on dual-chamber MFCs with different three-dimensional electrodes. Each MFC consisted of two Perspex frames (an anode chamber and a cathode chamber) separated by a cation exchange membrane (Ultrex CMI-7000, Membranes International Inc., Glen Rock, NJ, USA). The total volumes of the anode and cathode chambers were  $84.5 \text{ mL}$  ( $6.5 \text{ cm} \times 6.5 \text{ cm} \times 2.0 \text{ cm}$ ) and  $169 \text{ mL}$  ( $6.5 \text{ cm} \times 6.5 \text{ cm} \times 4.0 \text{ cm}$ ), respectively. The anode made of carbon felt ( $4.5 \text{ cm} \times 4.5 \text{ cm}$ , Hesen, Shanghai, China) was soaked for 24 h in acetone to eliminate potential contaminants from its surface [25]. The cathode chamber was filled with particle electrodes, and the contact and electron collection was performed through a graphite rod ( $6 \text{ cm}$  in length and  $0.8 \text{ cm}$  in diameter). Three different kinds of particle electrodes were used as cathodes: (1) activated carbon particle electrodes (ACPE), (2) carbon black particle electrodes (CBPE) and (3) graphite particle electrodes (GPE), these were labeled MFC-ACPE, MFC-CBPE and MFC-GPE. The net volume of MFC's cathode compartment was  $120 \text{ mL}$ . The anode was inoculated with wastewater collected from Taida Municipal Wastewater treatment plant in Tianjin. Wastewater was mixed with the growth media ( $770 \text{ mg L}^{-1}$  COD, pH 7.0), which consisted of  $1 \text{ g L}^{-1}$  acetate,  $50 \text{ mM}$  PBS ( $0.31 \text{ g L}^{-1} \text{ NH}_4\text{Cl}$ ,  $0.13 \text{ g L}^{-1} \text{ KCl}$ ,  $2.452 \text{ g L}^{-1} \text{ NaH}_2\text{PO}_4 \cdot \text{H}_2\text{O}$ ,  $4.576 \text{ g L}^{-1} \text{ Na}_2\text{HPO}_4$ ), a mineral solution and a vitamin solution [26]. The cathode chamber was fed with a  $50 \text{ mM}$   $\text{Na}_2\text{SO}_4$  solution and was continually subjected to aeration. In the start-up phase, an external resistor of  $1000 \Omega$  was used to connect the MFC circuit, and all MFCs were operated at temperature of  $30 \pm 0.5^\circ\text{C}$  in a controlled biochemical incubator. The voltages of the MFCs were recorded by a data acquisition system connected to a personal computer (PISO-813, ICP DAS Co., Ltd, China).

### 2.4. MFC tests and electrochemical analysis

Polarization and power density curves were used to evaluate the power density of the MFCs by varying the external resistance over a range of 10–5000 using a resistor box when the voltage output stayed steady. The power densities were normalized to the effective volume of the cathode chamber. The potentials of the anode and cathode were measured using a saturated calomel electrode (SCE,  $+0.242 \text{ V}$  vs. SHE) as the reference. Linear sweep voltammetry (LSV) measurements were tested by a potentiostat (CHI660D, ChenHua Instruments Co., Ltd., Shanghai, China) in  $50 \text{ mM}$  of  $\text{Na}_2\text{SO}_4$  at pH 7.0. Each particle electrode with a graphite rod was used as a working electrode, while a platinum sheet of  $1 \text{ cm}^2$  and an SCE were used as the counter and the reference electrodes. Before the measurements, the solution was saturated with oxygen. LSV was conducted from  $0.3 \text{ V}$  to  $-0.9 \text{ V}$  at a scan rate of  $1 \text{ mV s}^{-1}$  ( $30^\circ\text{C}$ ).

### 2.5. Chemical analysis

The concentrations of  $\text{H}_2\text{O}_2$  in the cathode chamber were determined by spectrophotometrical analysis according to the

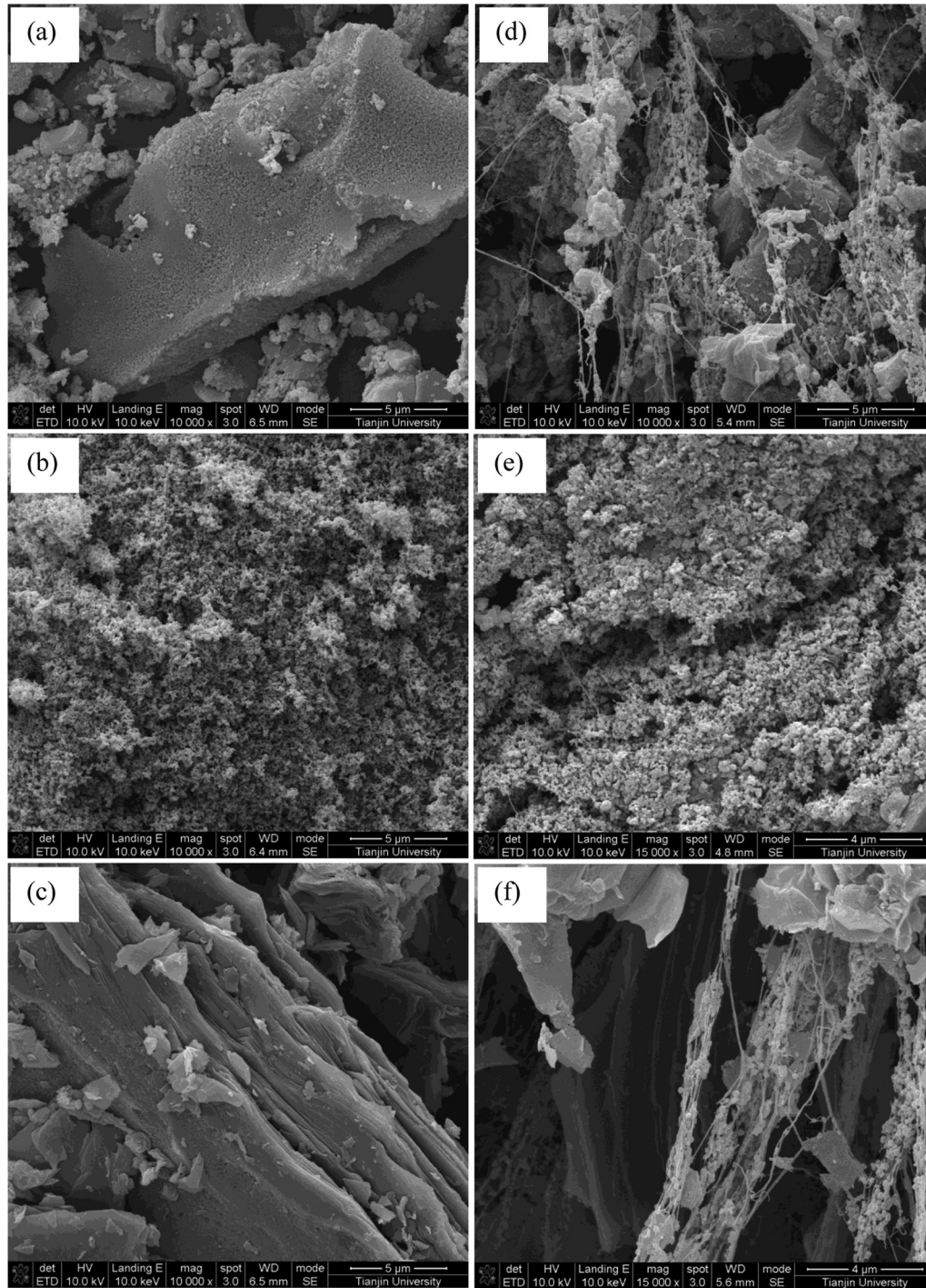


**Fig. 1.** SEM images of (a) AC powders, (b) CB powders and (c) graphite powders at a magnification of 10 K; SEM images of (d) AC-PTFE granules, (e) CB-PTFE granules and (f) graphite-PTFE granules made from corresponding carbon powders with PTFE binder at a magnification of 15 K.

titanium oxalate method [27]. The catholyte pH was measured by pH meter (PHSJ-3F, INESA Scientific Instrument Co. Ltd, Shanghai, China). The chemical oxygen demand (COD) was measured using DRB200 and DR2800 (Hash, USA). Coulombic efficiency was defined as the Coulombs ratio of the charge production and the anodic COD consumption [28], calculated using Equation (1). Faradic efficiency was defined as the cathodic  $\text{H}_2\text{O}_2$  production divided by the charge production [28], calculated according to Equation (2). COD conversion efficiency, defined as the proportion of cathodic  $\text{H}_2\text{O}_2$  production contained in the anodic COD consumption [16], was calculated using Equation (3).

$$C_{\text{Coulombic}}E = \frac{C}{C_{\text{COD}}} \quad (1)$$

$$C_{\text{Faradic}}E = \frac{C_{\text{H}_2\text{O}_2}}{C} \quad (2)$$

$$CE = C_{\text{Coulombic}}E \times C_{\text{Faradic}}E \quad (3)$$

where  $C_{\text{Coulombic}}E$  is the Coulombic efficiency (%),  $C_{\text{Faradic}}E$  is the current efficiency (%),  $CE$  is COD the conversion efficiency (%),  $\text{C}_{\text{H}_2\text{O}_2}$

(C) is the cumulative  $\text{H}_2\text{O}_2$  production expressed as the charge in Coulombs (based on  $2 \text{ mol e}^-$  consumed per mol of  $\text{H}_2\text{O}_2$  produced),  $C$  is the total Coulombs (C) obtained by integrating the current over time, and  $C_{\text{COD}}$  is the theoretical amount of the Coulombs (C), which is the cumulative COD consumption expressed as charge (based on  $8 \text{ mol e}^-$  produced per  $64 \text{ g COD}$  consumed).

### 3. Results and discussion

#### 3.1. Morphology and porosity of the carbon particles

The results of the morphologies for carbon powders and carbon-PTFE granules are given in Fig. 1. The SEM images, at a magnification of  $10 \text{ K}$  (Fig. 1(a)–(c)), show the random pore size distributions and interconnected pore systems in all three carbon powders. Also, the activated carbon powders and graphite powders have the appearance of a sheet-like morphology. The surface morphology of the three carbon-PTFE granules revealed by SEM images at a magnification of  $15 \text{ K}$  (Fig. 1(d)–(f)) shows that the tight and brawny PTFE fibers are present in the AC-PTFE granules and graphite-PTFE granules, but these are not observed clearly in the CB-PTFE granules.

Based on the  $\text{N}_2$  adsorption/desorption isotherms of the three carbon-PTFE granules shown in Fig. 2, the porous properties and pore size distribution were obtained; these are summarized in Table 1. The results indicate that the three carbon-PTFE granules had a wide pore size distribution. Isotherms of the three carbon-PTFE granules all belonged to type IV with a pronounced hysteresis at a higher  $P/P_0$ , caused by capillary condensation in mesopore structures [29]. The hysteresis loops of the AC-PTFE granules and graphite-PTFE granules were type H4. The shapes of the hysteresis loops confirmed that slit-like mesopores exist in the granules [30,31], corresponding to the morphology shown in the SEM images. However, the absorption volume of the graphite-PTFE granules was relatively low compared to that of the AC-PTFE granules, which could be expected, given the small surface area of the graphite-PTFE granules ( $46.9 \text{ m}^2 \text{ g}^{-1}$ ). The hysteresis loops of the CB-PTFE granules were of type H3, with a steeper shape, indicating a random pore distribution, an interconnected pore system, more mesopore, and probably macropore adsorption [32]. The data listed in Table 1 reveal that the CB-PTFE granules had a larger average pore size and a higher proportion of mesopore area to the total surface area ( $6.236 \text{ nm}$ ;  $51.51\%$ ) than the AC-PTFE granules ( $3.334 \text{ nm}$ ;  $64.20\%$ ) and the graphite-PTFE granules ( $5.233 \text{ nm}$ ;

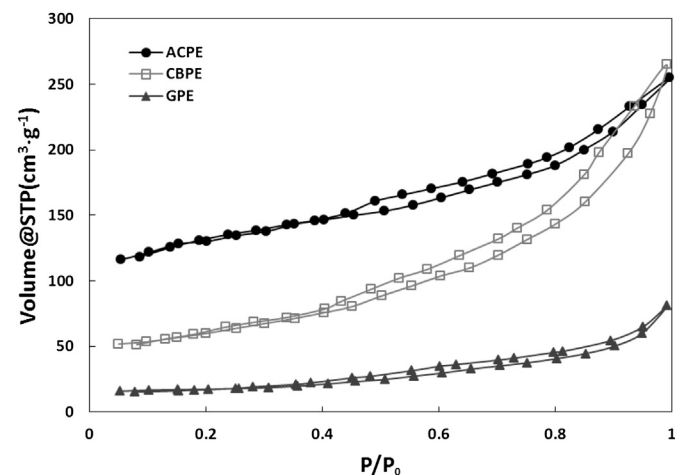


Fig. 2.  $\text{N}_2$  adsorption/desorption isotherms of AC-PTFE, CB-PTFE and graphite-PTFE granules.

Table 1

Data on the porous structural characteristics of the  $\text{N}_2$  adsorption/desorption isotherms of AC-PTFE, CB-PTFE and graphite-PTFE granules.

Sample	AC-PTFE	CB-PTFE	Graphite-PTFE
Specific surface area ( $\text{m}^2 \text{ g}^{-1}$ )	248.7	159.5	46.9
Micropore area ( $\text{m}^2 \text{ g}^{-1}$ )	90.6	57.1	18.7
Mesopore area ( $\text{m}^2 \text{ g}^{-1}$ )	128.1	102.4	28.2
Micropore volume ( $\text{cm}^3 \text{ g}^{-1}$ )	0.201	0.161	0.020
Mesopore area/total surface area (%)	51.51	64.20	60.13
Average pore diameter (nm)	3.334	6.236	5.233
BJH method desorption pore diameter (nm)	1.629	2.591	1.893

$60.13\%$ ). The findings clearly demonstrate that the particles under study were porous, had with a large surface area and had a three-dimensional network structure.

#### 3.2. Electrochemical analysis and MFC tests

The LSV of oxygen reduction on the cathodes in the  $0.05 \text{ mol L}^{-1} \text{ Na}_2\text{SO}_4$  solution deoxygenated and saturated with  $\text{O}_2$  was measured to evaluate the catalytic activity of the cathode toward oxygen reduction (Fig. 3). As the control, the LSV of hydrogen peroxide reduction on cathodes in  $0.05 \text{ mol L}^{-1} \text{ Na}_2\text{SO}_4$  solution with  $300 \mu\text{M H}_2\text{O}_2$  was measured (Fig. 3 inset). It was obvious that each voltammetric curve of the particle electrodes in the saturated  $\text{O}_2$  solution (curves (d), (e) and (f)) exhibited two reduction peaks, compared to each background curve recorded in the deoxygenated solution (curves (a), (b) and (c)), which proves that the three particle electrodes had a capability for electro-catalytic oxygen reduction. Upon the addition of  $300 \mu\text{M H}_2\text{O}_2$ , there was a linear increase in the cathodic peak current at  $-700 \text{ mV}$  (vs. SCE) that was observed (curves (d'), (e') and (f')). Thus, the first reduction peak at a less negative potential ( $-500 \text{ mV}$  vs. SCE) in curves (d), (e) and (f) was supposedly the two-electron reduction of oxygen to  $\text{H}_2\text{O}_2$  on the particle electrodes [15]. The second reduction peak in curves (d), (e) and (f) was found at a more negative potential ( $-700 \text{ mV}$  vs. SCE), which corresponds to a further two-electron reduction that generated water [15]. Curve (d) and curve (e) show that the oxygen reduction reaction began at a more positive potential and gained a higher peak current on the ACPE and the CBPE, indicating strong electro-activity in the presence of oxygen reduction and high transfer rate of change, which was in accordance with the sequence of power densities (see Fig. 4(a)). Moreover, the possible

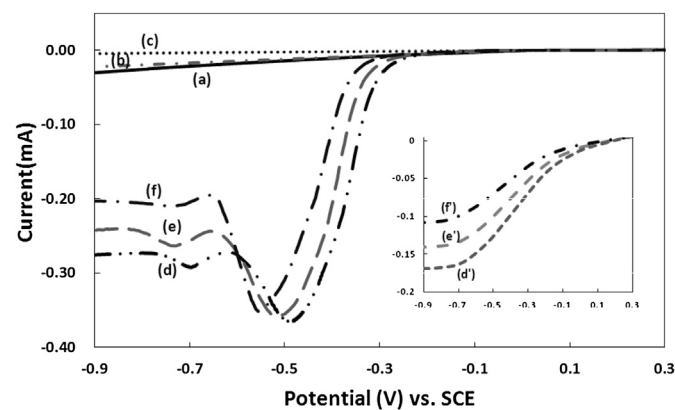


Fig. 3. Linear sweep voltammetry of particle electrodes in  $0.05 \text{ mol L}^{-1} \text{ Na}_2\text{SO}_4$  solution at a  $1 \text{ mV s}^{-1}$  scan rate. The ACPE (a), CBPE (b) and GPE (c) with deoxygenated solution; The ACPE (d), CBPE (e) and GPE (f) with oxygen saturated solution; The ACPE (d'), CBPE (e') and GPE (f') with  $300 \mu\text{M H}_2\text{O}_2$  (inset).

accumulation of  $\text{H}_2\text{O}_2$  resulted in a negative shift of reduction potentials, as follows: ACPE (d) > CBPE (e) > GPE (f), based on the Nernst equation, indicating that GPE may have the best performance on  $\text{H}_2\text{O}_2$  production.

The polarization and power density curves for the MFCs using the ACPE, the CBPE and the GPE as cathodes are compared in Fig. 4. According to the power curve, the MFC-ACPE produced the highest maximum power density of  $5.64 \text{ W m}^{-3}$ , followed by the MFC-CBPE of  $3.88 \text{ W m}^{-3}$  and then the MFC-GPE of  $2.20 \text{ W m}^{-3}$ , all at an external resistance of  $150 \Omega$  (Fig. 4(a)). The open circuit voltages (OCV) of the MFC-ACPE, the MFC-CBPE, and the MFC-GPE were  $0.561 \text{ V}$ ,  $0.556 \text{ V}$  and  $0.475 \text{ V}$ , respectively (Fig. 4(b)). The OCV of the MFC-ACPE and the MFC-CBPE was 18% and 17% higher than that of the MFC-GPE. The losses of OCV can be attributed to the mixed cathodic potential caused by the competing two electrons ORR, which produced  $\text{H}_2\text{O}_2$  to complete four electrons ORR ( $\sim 0.5 \text{ V}$  more positive than two electrons ORR in thermodynamic equilibrium potential). They were also larger than those previous  $\text{H}_2\text{O}_2$ -producing MFCs using two-dimensional electrode ( $0.340 \text{ V}$  [28] and  $0.440 \text{ V}$  [14]). The activation polarization loss was not obvious in all of the MFCs. Since the anode potentials of all of the MFCs were the same (Fig. 4(b)), differences in all of three MFCs can be attributed to the cathodes. AC-PTFE granules and CB-PTFE granules with a higher specific surface area produced an excellent power output. Additionally, the oxygen diffused first to the surface of the macropores and mesopores, and then to the inner micropores [32]. Thus, more micropores in the AC-PTFE granules can provide additional ORR sites and result in a better performance of the MFC than CB-PTFE

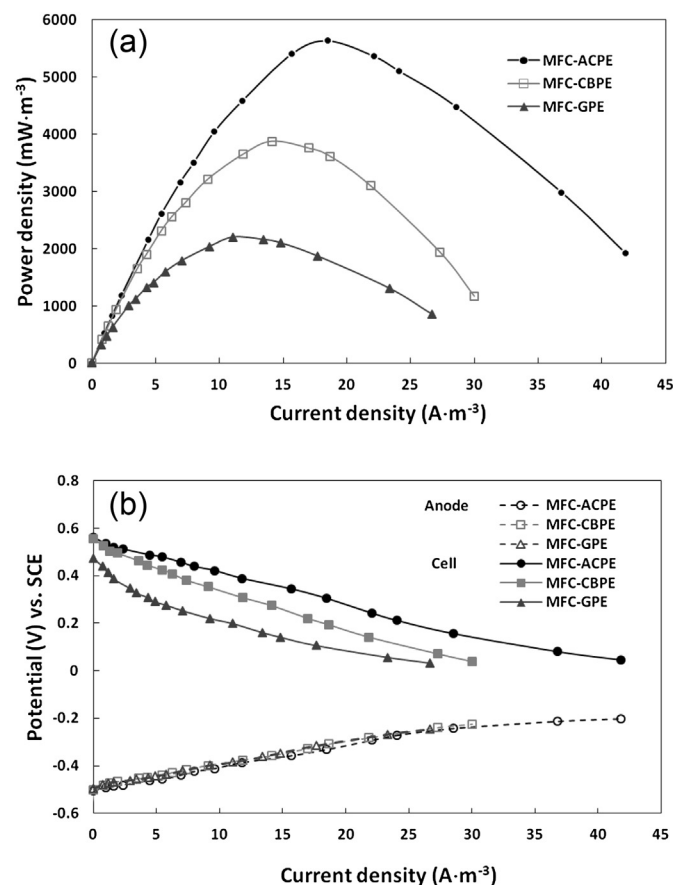


Fig. 4. (a) Power density (normalized to the cathode effective) as a function of the current density in MFCs using the ACPE, the CBPE and the GPE; (b) Electrode potentials for the MFCs using the ACPE, the CBPE and the GPE.

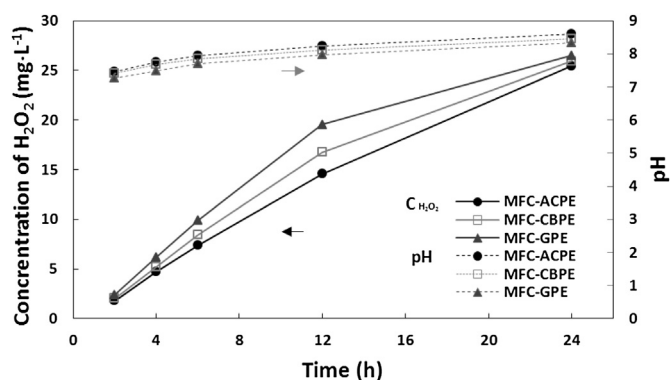


Fig. 5.  $\text{H}_2\text{O}_2$  concentration and pH versus time in the MFC-ACPE, the MFC-CBPE, and the MFC-GPE with an external resistance of  $1000 \Omega$ .

granules can achieve. In comparison, the graphite-PTFE granules had the smallest surface area; therefore, the MFC-GPE had the lowest maximum power density.

### 3.3. Performance of $\text{H}_2\text{O}_2$ production and COD removal

$\text{H}_2\text{O}_2$  production was investigated in the stable operation period of the MFCs using the ACPE, the CBPE and the GPE with an external resistance of  $1000 \Omega$  for 24 h.  $\text{H}_2\text{O}_2$  concentrations were measured after 2 h, 4 h, 6 h, 12 h and 24 h, as shown in Fig. 5. MFCs using three-dimensional electrode produced a larger concentration of  $\text{H}_2\text{O}_2$  than has been previously reported (about  $15\text{--}20 \text{ mg L}^{-1}$ ) for MFCs with flat cathode in MFCs [14,33]. Within 24 h, the highest concentration of  $26.56 \text{ mg L}^{-1}$  was produced in the MFC-GPE, followed by  $25.92 \text{ mg L}^{-1}$  in the MFC-CBPE and  $25.44 \text{ mg L}^{-1}$  in the MFC-ACPE. The trend was reversed compared to that of power density because the two-electron ORR pathway led to a great loss of thermodynamic equilibrium potential. For example, the thermodynamic equilibrium potential of  $\text{H}_2\text{O}_2$  production is  $0.26 \text{ V}$ , which is 67% lower than the  $0.78 \text{ V}$  of  $\text{H}_2\text{O}$  production at a pH of 7.5 (vs. standard hydrogen electrode) [34]. Hence,  $\text{H}_2\text{O}_2$  as the oxygen reduction intermediate was further cathodic reduced to  $\text{H}_2\text{O}$  in the MFC-ACPE and the MFC-CBPE, which led to a higher cathodic potential and a stronger power density. Furthermore, the reduction of  $\text{H}_2\text{O}_2$  on the porous surface of the ACPE and the CBPE could lead to a greater loss of  $\text{H}_2\text{O}_2$  than with the GPE according to the LSV results. The  $\text{H}_2\text{O}_2$  concentration attained an approximately linear growth during the first 12 h and then underwent a relatively slow increase over the next 12 h, especially in the MFC-GPE. A possible reason for this reduction is that the considerable accumulation of  $\text{H}_2\text{O}_2$  in the catholyte may have slowed down the oxygen reduction rate. This phenomenon was not obvious in the MFC-ACPE, because  $\text{H}_2\text{O}_2$  was quickly reduced into water to avoid the over-accumulation of hydrogen peroxide. The change of pH in catholyte with time was measured (Fig. 5), shown no obvious difference for the three MFCs. The phosphate buffer solution contained cationic alkali species (e.g.,  $\text{Na}^+$ ,  $\text{K}^+$ ), which could be transported by the cation exchange membrane from the anode to the cathode, resulted in a light pH increase of catholyte in the three MFCs [17].  $\text{H}_2\text{O}_2$  is relatively stable in the catholyte in its protonated state at  $\text{pH} < 9$ , since the  $\text{pK}_a$  of  $\text{H}_2\text{O}_2$  is 11.62 at  $25^\circ\text{C}$  [35].

COD removals for the MFC-ACPE, the MFC-CBPE, and the MFC-GPE with an external resistance of  $1000 \Omega$  approached 34%, 33%, and 31%, respectively, after 24 h (Table 2), suggesting that high current correlated with high degradation efficiency. The  $C_{\text{Coulombic}}$ Es were low, which contributed to poor utilization of the large free space in the anode chamber relative to the anode volume,

**Table 2**Performance for H<sub>2</sub>O<sub>2</sub> production and COD removal in MFCs using the ACPE, the CBPE and the GPE with various external resistances.

MFCs	External resistance ( $\Omega$ )	COD removal (%)	H <sub>2</sub> O <sub>2</sub> concentration (mg L <sup>-1</sup> )	Current density <sup>a</sup> (A m <sup>-3</sup> )	C <sub>Coulombic</sub> E (%)	C <sub>Faradic</sub> E (%)	CE (%)
MFC-ACPE	1000	34	25.44	3.60	14	46	7
	600	38	37.73	5.31	19	47	9
	300	52	57.65	8.02	21	47	10
	150	64	82.87	11.05	23	49	11
	100	71	101.54	13.44	25	50	12
	20	87	164.33	21.95	33	50	16
MFC-CBPE	1000	33	25.92	3.46	14	49	7
	600	35	37.89	4.95	18	50	9
	300	49	58.65	7.14	19	54	10
	150	63	86.33	10.25	21	55	12
	100	70	110.23	12.81	24	57	14
	20	85	171.18	20.32	31	56	17
MFC-GPE	1000	31	26.56	3.08	13	57	8
	600	34	38.35	4.29	17	59	10
	300	46	60.95	6.18	18	65	11
	150	61	98.51	9.29	20	67	14
	100	68	121.31	11.33	22	70	16
	20	84	196.50	18.41	29	70	20

<sup>a</sup> The steady current density on the cathode electrode (normalized to the effective volume of the cathode).

but this phenomenon lies beyond the scope of this paper, which is devoted to the performance of the cathode. The  $C_{\text{Coulombic}}E$ s of the three MFCs observed were close to each other, indicating that the performance of these anodes was similar, as shown in the polarization curves. The slight differences in the  $C_{\text{Coulombic}}E$  in the MFC-ACPE, the MFC-CBPE, and the MFC-GPE can be associated with differences in the MFC current density. The  $C_{\text{Faradic}}E$  of the MFC-GPE with a loading resistor of 1000  $\Omega$  reached 57%, followed by 49% for the MFC-CBPE and 46% for the MFC-ACPE, which is consistent with the trend of H<sub>2</sub>O<sub>2</sub> concentration, indicating that the cathodic reduction of hydrogen peroxide had a substantial effect on the  $C_{\text{Faradic}}E$ s. The COD conversion efficiency was influenced by both the Coulombic efficiency and the Faradic efficiency, which represented the performance of anode and cathode, respectively. In terms of cell performance for H<sub>2</sub>O<sub>2</sub> production, the MFC-GPE with a loading resistor of 1000  $\Omega$  had a higher CE of 7.5% compared to 6.8% for the MFC-CBPE and 6.5% for the MFC-ACPE, which was contrary to electricity generation performance, because the AC-PTFE and CB-PTFE granules with more micropores facilitated the ORR process and caused further reduction of H<sub>2</sub>O<sub>2</sub>, leading to less H<sub>2</sub>O<sub>2</sub> production in the MFCs.

Though the MFCs using three-dimensional electrodes obtained a higher yield of H<sub>2</sub>O<sub>2</sub>, the concentration was still sparse compared with other studies on H<sub>2</sub>O<sub>2</sub> synthesis using chemical fuel cells [9–11]. In an effort to maximize H<sub>2</sub>O<sub>2</sub> production, the performance of H<sub>2</sub>O<sub>2</sub> production in the MFC-ACPE, the MFC-CBPE, and the MFC-GPE was tried different external resistances; the results are compared in Table 2. For the three MFCs, when the current density increased due to a decrease in external resistance, the production rate of H<sub>2</sub>O<sub>2</sub> all rose. However, with a same external resistance, the MFC-ACPE and the MFC-CBPE generated a little larger current density than the MFC-GPE. The difference in current density of the three MFCs was caused by the difference of electrochemical property in cathode materials, which also affected the performance of H<sub>2</sub>O<sub>2</sub> production. Thus, a relatively smaller external resistance or a higher current leads to better performance of H<sub>2</sub>O<sub>2</sub> production for a given cathode. The anodic acetate degradation rate was also affected by the current density of the MFCs. For example, The CEs of the three MFCs with a 20  $\Omega$  resistor were more than twice that of the CE with a 1000  $\Omega$  resistor.  $C_{\text{Coulombic}}E$  improved as external resistance declined, which shows that external resistance had an impact on the anode performance as well [14]. Following an increase in current density, not only did the H<sub>2</sub>O<sub>2</sub> concentration rise, but  $C_{\text{Faradic}}E$  also increased. However, the  $C_{\text{Faradic}}E$  in the MFC-ACPE,

the MFC-CBPE, and the MFC-GPE with a loading resistor of 20  $\Omega$  was slightly lower than that with a loading resistor of 100  $\Omega$ , possibly because the transfer of oxygen limited the further increase of current density. Thus, a portion of the H<sub>2</sub>O<sub>2</sub> was utilized as an alternative electron acceptor. Furthermore, the CE was increased along with the increase in current density. Particularly, when the MFC-GPE was operated at an external resistance of 20  $\Omega$ , the concentration of H<sub>2</sub>O<sub>2</sub> reached 196.50 mg L<sup>-1</sup> at a rate of 10.15 mg L<sup>-1</sup> h<sup>-1</sup> for the first 12 h and 6.23 mg L<sup>-1</sup> h<sup>-1</sup> for the last 12 h, which was higher than the 6.57 mg L<sup>-1</sup> h<sup>-1</sup> reported previously [14]. COD degradation efficiency reached 84%.  $C_{\text{Coulombic}}E$ ,  $C_{\text{Faradic}}E$ , and CE were 29%, 70%, and 20%, respectively. MFC-GPE using three-dimensional electrode with an external resistor of 20  $\Omega$  performed better in terms of H<sub>2</sub>O<sub>2</sub> production and COD removal.

#### 4. Conclusion

Three-dimensional electrode bioelectrochemical systems can efficiently degrade organic matter and generate H<sub>2</sub>O<sub>2</sub>. Electrochemical analysis indicated that the two-electron reaction for oxygen reduction was superior for the GPE. The MFC-ACPE and the MFC-CBPE showed better performance on power output but had a lower H<sub>2</sub>O<sub>2</sub> yield compared to the MFC-GPE because of a further cathodic two-electron reduction of H<sub>2</sub>O<sub>2</sub>. A relatively high current had a positive impact on cathodic H<sub>2</sub>O<sub>2</sub> generation and anodic organics degradation for each MFC. When the MFC-GPE operated under an external resistance of 20  $\Omega$  after 24 h, H<sub>2</sub>O<sub>2</sub> concentration reached 196.50 mg L<sup>-1</sup>, together with 84% COD removal. Coulombic efficiency, Faradic efficiency and COD conversion efficiency were 29%, 70%, and 20%, respectively.

#### Acknowledgments

This research work was financially supported by the National Natural Science Foundation of China (No. 51208352), the Tianjin Research Program of Application Foundation and Advanced Technology (No. 13JCQNJC09100) and Independent Innovation Research Fund of Tianjin University (No. 2013XQ-0042).

#### References

- [1] H. Liu, R. Ramnarayanan, B.E. Logan, Environ. Sci. Technol. 38 (2004) 2281–2285.
- [2] H. Wang, Z.J. Ren, Biotechnol. Adv. 31 (2013) 1796–1807.

- [3] B.E. Logan, B. Hamelers, R.A. Rozendal, U. Schröder, J. Keller, S. Freguia, P. Aelterman, W. Verstraete, K. Rabaey, *Environ. Sci. Technol.* 40 (2006) 5181–5192.
- [4] F. Zhao, F. Harnisch, U. Schroeder, F. Scholz, P. Bogdanoff, I. Herrmann, *Environ. Sci. Technol.* 40 (2006) 5193–5199.
- [5] P. Clauwaert, P. Aelterman, T.H. Pham, L. De Schampelaire, M. Carballa, K. Rabaey, W. Verstraete, *Appl. Microbiol. Biotechnol.* 79 (2008) 901–913.
- [6] R. Hage, A. Lienke, *Angew. Chem. Int. Ed. Engl.* 45 (2005) 206–222.
- [7] G. Ersoz, S. Atalay, *J. Adv. Oxid. Technol.* 16 (2013) 286–291.
- [8] J.M. Campos-Martin, G. Blanco-Brieva, J.L.G. Fierro, *Angew. Chem.-Int. Ed.* 45 (2006) 6962–6984.
- [9] D. Pletcher, *Acta Chem. Scand.* 53 (1999) 745–750.
- [10] I. Yamanaka, T. Onisawa, T. Hashimoto, T. Murayama, *Chemosuschem* 4 (2011) 494–501.
- [11] I. Yamanaka, T. Onisawa, S. Takenaka, K. Otsuka, *Angew. Chem.-Int. Ed.* 42 (2003) 3653–3655.
- [12] R.A. Rozendal, T.H.J.A. Sleutels, H.V.M. Hamelers, C.J.N. Buisman, *Water Sci. Technol.* 57 (2008) 1757–1762.
- [13] O. Scialdone, A. Galia, S. Sabatino, *Electrochem. Commun.* 26 (2013) 45–47.
- [14] L. Fu, S.-J. You, F.-I. Yang, M.-m. Gao, X.-h. Fang, G.-q. Zhang, *J. Chem. Technol. Biotechnol.* 85 (2010) 715–719.
- [15] C.-H. Feng, F.-B. Li, H.-J. Mai, X.-Z. Li, *Environ. Sci. Technol.* 44 (2010) 1875–1880.
- [16] L. Zhuang, S. Zhou, Y. Yuan, M. Liu, Y. Wang, *Chem. Eng. J.* 163 (2010) 160–163.
- [17] S.-J. You, J.-Y. Wang, N.-Q. Ren, X.-H. Wang, J.-N. Zhang, *Chemosuschem* 3 (2010) 334–338.
- [18] X. Wu, X. Yang, D. Wu, R. Fu, *Chem. Eng. J.* 138 (2008) 47–54.
- [19] W. Kong, B. Wang, H. Ma, L. Gu, *J. Hazard. Mater.* 137 (2006) 1532–1537.
- [20] L. Wei, S. Guo, G. Yan, C. Chen, X. Jiang, *Electrochim. Acta* 55 (2010) 8615–8620.
- [21] H. Wang, M. Davidson, Y. Zuo, Z. Ren, *J. Power Sources* 196 (2011) 5863–5866.
- [22] Z. He, *Environ. Sci. Technol.* 47 (2013) 332–333.
- [23] Y. Mu, K. Rabaey, R.A. Rozendal, Z. Yuan, J. Keller, *Environ. Sci. Technol.* 43 (2009) 5137–5143.
- [24] H. Dong, H. Yu, X. Wang, Q. Zhou, J. Feng, *Water Res.* 46 (2012) 5777–5787.
- [25] X. Wang, S. Cheng, Y. Feng, M.D. Merrill, T. Saito, B.E. Logan, *Environ. Sci. Technol.* 43 (2009) 6870–6874.
- [26] D.R. Lovley, E.J. Phillips, *Appl. Environ. Microbiol.* 54 (1988) 1472–1480.
- [27] O. Modin, K. Fukushima, *Water Sci. Technol.: J. Int. Assoc. Water Pollut. Res.* 66 (2012) 831–836.
- [28] R.A. Rozendal, E. Leone, J. Keller, K. Rabaey, *Electrochem. Commun.* 11 (2009) 1752–1755.
- [29] R. Pierotti, J. Rouquerol, *Pure Appl. Chem.* 57 (1985) 603–619.
- [30] S. Kumagai, H. Ishizawa, Y. Aoki, Y. Toida, *Chem. Eng. J.* 156 (2010) 270–277.
- [31] Y. Matsuo, Y. Sakai, T. Fukutsuka, Y. Sugie, *Carbon* 47 (2009) 804–811.
- [32] H. Dong, H. Yu, X. Wang, *Environ. Sci. Technol.* 46 (2012) 13009–13015.
- [33] L. Zhuang, S. Zhou, Y. Li, T. Liu, D. Huang, *J. Power Sources* 195 (2010) 1379–1382.
- [34] S.C. Popat, D. Ki, B.E. Rittmann, C.I. Torres, *Chemosuschem* 5 (2012) 1071–1079.
- [35] Z.M. Qiang, J.H. Chang, C.P. Huang, *Water Res.* 36 (2002) 85–94.